Influence of Nd^{3+} concentration on its optical absorption and luminescence properties in potassium borate glass

Y. C. Ratnakaram[*,1], **Md. Abdul Altaf**[1], **R. P. S. Chakradhar**[2], **J. L. Rao**[3], and **J. Ramakrishna**[2]

[1] Department of Physics, S. V. U. P. G. Centre, Kavali-524201, A.P, India
[2] Department of Physics, Indian Institute of Science, Bangalore-560 012, India
[3] Department of Physics, S. V. University, Tirupathi-517502, A.P, India

PACS 71.55.Jv, 78.40.Pg, 78.55.Hx

Spectroscopic and laser properties of Nd^{3+} doped potassium borate glass have been studied for different Nd^{3+} concentrations ranging from 0.5 to 2.0 mol%. From the absorption spectra, optical band gaps (E_{opt}) and various spectroscopic parameters (E^1, E^2, E^3, ξ_{4f} and α) are determined. Using Judd-Ofelt intensity parameters Ω_2, Ω_4 and Ω_6, radiative lifetimes (τ_R), branching ratios (β) and integrated absorption cross sections (Σ) have been calculated for certain excited states of Nd^{3+} for all the Nd^{3+} concentrations. From the spectral profiles of the hypersensitive transition, it is observed that there is slight change in the environment of Nd^{3+} ion in different concentrations of Nd^{3+} doped potassium borate glass. The radiative lifetimes (τ_R) for certain excited levels are minimum when the concentration is high. From the emission spectra, peak wavelengths (λ_p), effective line widths ($\Delta\lambda_{eff}$) and stimulated emission cross-sections (σ_p) have been obtained for the three transitions $^4F_{3/2} \rightarrow {}^4I_{9/2}$, $^4F_{3/2} \rightarrow {}^4I_{11/2}$ and $^4F_{3/2} \rightarrow {}^4I_{13/2}$ of Nd^{3+} and are compared for different concentrations.

1 Introduction

Glasses are attractive materials for industrial applications, as they can be cast in large, optically homogeneous pieces. Rare earth doped glasses have been widely studied for optical telecommunication [1] and laser technology [2]. The effect of host matrix on the local environment of a given rare earth cation with its first nearest neighbour anions can be elucidated with Judd-Ofelt [3, 4] theory using optical absorption spectra. Binnemans et al. [5] gave optical properties of Nd^{3+} doped fluorophosphate glasses. Li et al. [6] reported the spectroscopy of neodymium (III) in alumino-borosilicate glasses. Spectroscopic properties of Nd-doped glass for 944 nm laser emission have been given by Lu and Dutta [7]. Naftaly and Jha [8] studied Nd^{3+} doped fluoroaluminate glasses for 1.3 μm amplifier. Das Mohapatra [9] studied the spectroscopy of Nd^{3+} and the effect of Ce^{3+} ion impurity on its spectroscopic properties in calcium metaphosphate glass. Ravikanth kumar and Bhatnagar [10] studied the effect of modifier ions on the covalency of Nd^{3+} ions in cadmium borate glasses.

In the present work, we report the spectroscopic and laser properties of Nd^{3+} doped potassium borate glass in different Nd^{3+} concentrations. The Judd-Ofelt theory has been applied to interpret the

[*] Corresponding author: e-mail: Ratnakaram_yc@yahoo.co.in, Tel.: 091-08626-44271

local environment and bond covalency, studying changes in the experimentally fitted Judd-Ofelt intensity parameters. This article also gives information about the relation between intensity of the hypersensitive transition and intensity parameters. Our main interest in the present study is to examine the variation of optical band gaps, Judd-Ofelt intensity parameters, peak to peak intensity ratios, the shape of the spectral profiles of emission spectra and emission properties with various Nd^{3+} concentrations. In the recent past, we have reported the results on spectroscopy of Nd^{3+} doped different chlorophosphate glasses and borate glasses [11, 12].

2 Experimental

The rare earth doped borate glasses were prepared using appropriate amounts of H_3BO_3, K_2CO_3 and Nd_2O_3 of high purity (99.99%). The raw materials were thoroughly mixed and ground in an agate mortar in 10 g batches. The mixture was then melted in a porcelain crucible at 850 °C. The melts were kept at their melting temperatures for about 30 min with occasional stirring to ensure homogeneity. Then the melt was quickly quenched between two tiles (optically polished ceramic slabs). Glass samples of about 1 mm thickness and 1 cm diameter were obtained. Special care was taken to see that these glass discs were not exposed to moisture by keeping in liquid paraffin containers. Optically transparent glasses were selected for optical studies. The systems studied in the present work are $80H_3BO_3 + (20-x)K_2CO_3 + xNd_2O_3$ ($x = 0.5$, 1.0, 1.5 and 2.0).

The glass densities were determined by using the Archimedes principle with xylene as the immersion liquid. The refractive indices of the above glasses were measured on an Abbe refractometer using 1-mono-bromonaphthalene as adhesive coating. Optical absorption spectra of these samples were recorded using Hitachi U-3400 spectrophotometer. The luminescence spectra were taken on Midac-FT photoluminescence spectrophotometer.

3 Theory

The measurement of optical absorption and the absorption edge is important in connection with the theory of the electronic structure of amorphous materials. The position of absorption edge and hence the value of optical band gap was found to depend on the glass composition. The absorption edge of non-metallic materials gives a measure of energy gap. Mott and Davis [13] gave the following forms of absorption co-efficient $\alpha(\omega)$ as a function of photon energy $\hbar\omega$ for direct and indirect transitions.

For direct transitions

$$\alpha(\omega) = B(\hbar\omega - E_{\text{opt}})^n/\hbar\omega\,, \tag{1}$$

where $n = 1/2$ for allowed transitions, B is a constant and E_{opt} is the direct optical band gap.

For indirect transitions

$$\alpha(\omega) = B(\hbar\omega - E_{\text{opt}})^n/\hbar\omega\,, \tag{2}$$

where $n = 2$ for allowed transitions and E_{opt} is the indirect optical band gap. Using the above two equations, one can find the optical energy band gaps (E_{opt}) for direct and indirect transitions.

The transition energies for Nd^{3+} were fitted with energy parameters using the Hamiltonian

$$H = H_{\text{e}} + H_{\text{so}} + H'\,, \tag{3}$$

where H_{e} corresponds to interaction between pairs of electrons expressed in terms of the Racah parameters (E^1, E^2, E^3), H_{so} and H' signify spin-orbit coupling (ξ) and configuration interactions (α) respectively. The energy, E_J, of the J-th level may be written in a Taylor's series expansion [14] as

$$E_J = E_{0J} + \sum_{k=1}^{3} \frac{\mathrm{d}E_J}{\mathrm{d}E^k}\,\Delta E^k + \frac{\mathrm{d}E_J}{\mathrm{d}\xi}\,\Delta\xi + \frac{\mathrm{d}E_J}{\mathrm{d}\alpha}\,\Delta\alpha + \ldots\,, \tag{4}$$

where E_{0J} is the zero order energy of the J-th level and dE_J/dE^k, $dE_J/d\xi$ and $dE_J/d\alpha$ are partial derivatives. The method of calculating the various spectroscopic parameters (E^1, E^2, E^3, ξ_{4f} and α), experimental and calculated transition energies are described in our earlier papers [11, 12].

The experimental oscillator strengths (f_{exp}) were calculated as described earlier [11]. In the present work, the intensities of all the absorption bands have been measured using the area method. The uncertainties in the measurement of experimental oscillator strengths were estimated to be $\pm 5\%$ for intense transitions and $\pm 10\%$ for weak transitions. According to Judd-Ofelt theory [11] the oscillator strength of a transition between an initial J manifold $(S, L)\,J$ and a final J' manifold $(S', L')\,J'$ is given by

$$f_{cal}(aJ, bJ') = \sum_{\lambda=2,4,6} T_\lambda \nu |\langle (SL)\,J \| U^\lambda \| (S'L')\,J' \rangle|^2 , \tag{5}$$

where ν is the mean energy of the transition, $\|U^\lambda\|^2$ represents the square of the reduced matrix elements of the unit tensor operator $\|U^\lambda\|$ connecting the initial and final states. The matrix elements are calculated in the intermediate coupling approximations. Because of the electrostatic shielding of the 4f electrons by the closed 5p shell electrons, the matrix elements of the unit tensor operator between two energy manifolds in a given rare earth ion do not vary significantly when it is incorporated in different hosts. Therefore, the squared reduced matrix elements of the unit tensor operator $\|U^\lambda\|^2$ are taken from the literature [11].

Substituting the 'f_{exp}' for 'f_{cal}' and using the squared reduced matrix elements, T_λ parameters are obtained using least square fit method. The three intensity parameters Ω_2, Ω_4 and Ω_6, which are characteristic of a given rare earth ion in a given matrix are obtained from

$$\Omega_\lambda = (2J+1)\,T_\lambda \left[9.218 \times 10^{-12} \times \frac{9n}{(n^2+2)^2} \right] . \tag{6}$$

From these Ω_λ parameters, radiative transition probabilities (A), radiative lifetimes (τ_R), branching ratios (β) and integrated absorption cross sections (Σ) have been calculated.

4 Results and discussion

4.1 Optical band gaps

The optical band gap values (E_{opt}) are measured for both direct and indirect transitions for different concentrations of Nd^{3+} doped potassium borate glasses. These values are 2.62, 2.71, 2.55 and 2.15 eV for direct transitions and 3.31, 3.30, 2.99 and 2.91 eV for indirect transitions for 0.5, 1.0, 1.5 and 2.0 mol% of Nd^{3+} concentrations. It is observed that the optical band gap values decrease with the increase of rare earth ion concentration for indirect transitions. For direct transitions also, E_{opt} values are decreasing with increasing Nd^{3+} concentration. But for 1.0 mol% of Nd^{3+}, it was not followed.

4.2 Energy levels

Optical absorption spectrum of Nd^{3+} doped potassium borate glass with 1.5 mol% of Nd^{3+} is shown in Fig. 1. Though the spectral intensities are slightly changes with concentration, the shape of the spectra is similar for all the concentrations. Hence they are not shown. The experimental and calculated energies of certain excited levels of Nd^{3+} ion are presented in Table 1 for four concentrations. The rms deviations between the experimental and calculated energies are reasonable. The Racah (E^1, E^2 and E^3), spin-orbit (ξ_{4f}) and configuration interaction (α) parameters obtained for all the glasses are also presented in Table 1. The hydrogenic ratios (E^1/E^3) and (E^2/E^3), which indicate the radial properties of Nd^{3+} are more or less the same for all the glasses indicating that the radial properties of Nd^{3+} ion are not affected by varying the Nd^{3+} concentration.

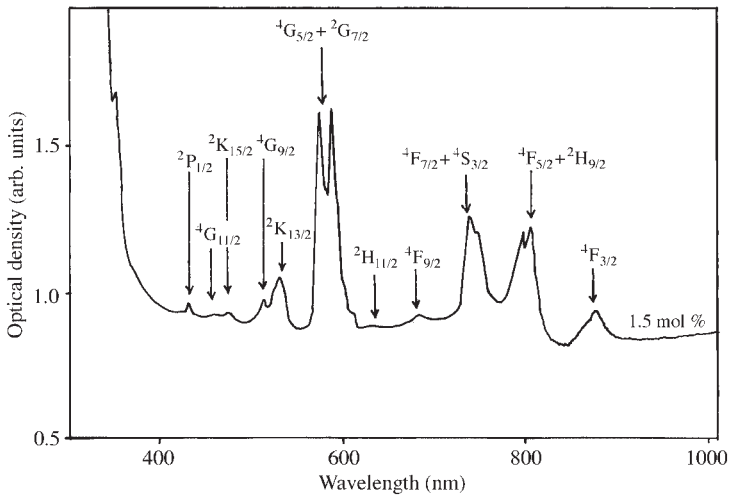

Fig. 1 Optical absorption spectrum of Nd^{3+} doped potassium borate glass with 1.5 mol% Nd^{3+} concentration.

4.3 Spectral intensities

The experimental (f_{exp}) and calculated (f_{cal}) spectral intensities of different absorption bands of Nd^{3+} have been obtained and are presented in Table 2. The rms deviations between the experimental and calculated values are very low confirming the validity of Judd-Ofelt theory. The spectral intensities of most of the bands are low in glasses containing 0.5 mol% of Nd^{3+} and are higher in glasses contain-

Table 1 Experimental (E_{exp}) and calculated (E_{cal}) energies and various spectroscopic parameters of Nd^{3+} in potassium borate glass with different concentrations (energy values are in cm^{-1}).

Serial No.	Energy level	0.5 mol%		1.0 mol%		1.5 mol%		2.0 mol%	
		E_{exp}	E_{cal}	E_{exp}	E_{cal}	E_{exp}	E_{cal}	E_{exp}	E_{cal}
1.	$^4F_{3/2}$	11355	11380	11415	11388	11416	11408	11402	11333
2.	$^4F_{5/2}$, $^2H_{9/2}$	12515	12465	12443	12468	12490	12488	12411	12422
3.	$^4F_{7/2}$, $^4S_{3/2}$	13484	13430	13548	13444	13541	13455	13439	13422
4.	$^4F_{9/2}$	14618	14741	14605	14757	14609	14750	14650	14752
5.	$^2H_{11/2}$	15881	–	15975	–	15861	–	15937	–
6.	$^4G_{5/2}$, $^2G_{7/2}$	17204	17173	17257	17240	17198	17184	17083	17140
7.	$^2K_{13/2}$, $^4G_{7/2}$	18763	18732	18827	18928	18784	18684	18977	18962
8.	$^4G_{9/2}$	19427	19301	19526	19398	19442	19323	19457	19417
9.	$^2K_{15/2}$, $^2G_{9/2}$, $^2D_{3/2}$	20767	20852	21011	21032	21122	20781	21046	21056
10.	$^4G_{11/2}$	21723	21683	21799	21733	21719	21665	21714	21662
11.	$^2P_{1/2}$	23168	23146	23195	23172	23120	23099	23099	23092
rms deviation		±98		±117		±185		±68	
E^1		5027.5		5056.5		4997.2		5029.6	
E^2		27.6		27.2		26.9		25.9	
E^3		489.2		492.8		488.7		489.3	
ξ_{4f}		921.9		916.8		915.2		918.7	
α		3.2		5.2		1.4		4.3	
E^1/E^3		10.3		10.3		10.2		10.3	
E^2/E^3		0.056		0.055		0.055		0.053	

Table 2 Experimental (f_{exp}) and calculated (f_{cal}) spectral intensities of Nd^{3+} doped potassium borate glass with different concentrations; all the transitions are from the ground $^4I_{9/2}$.

Serial No.	Excited level	0.5 mol%		1.0 mol%		1.5 mol%		2.0 mol%	
		f_{exp}	f_{cal}	f_{exp}	f_{cal}	f_{exp}	f_{cal}	f_{exp}	f_{cal}
1.	$^4F_{3/2}$	1.390	1.596	1.418	1.649	2.209	2.379	3.387	3.134
2.	$^4F_{5/2}$, $^2H_{9/2}$	5.264	5.118	5.767	5.570	5.317	5.989	7.677	8.048
3.	$^4F_{7/2}$, $^4S_{3/2}$	5.000	5.141	5.701	5.862	5.748	5.385	7.617	7.371
4.	$^4F_{9/2}$	0.674	0.412	0.411	0.458	0.864	0.448	1.165	0.614
5.	$^2H_{11/2}$	0.083	0.110	0.101	0.124	0.085	0.123	0.124	0.169
6.	$^4G_{5/2}$, $^2G_{7/2}$	22.997	23.012	20.940	20.947	19.407	19.511	24.428	24.409
7.	$^2K_{13/2}$, $^4G_{7/2}$	3.842	3.786	3.863	3.760	6.026	4.263	5.387	5.630
8.	$^4G_{9/2}$	1.566	1.108	1.432	1.161	2.219	1.427	2.764	1.895
9.	$^2K_{15/2}$, $^2G_{9/2}$, $^2D_{3/2}$	0.858	0.421	1.121	0.449	1.088	0.587	1.207	0.779
10.	$^4G_{11/2}$	0.743	0.147	0.639	0.161	0.845	0.182	1.152	0.245
11.	$^2P_{1/2}$	0.176	0.444	0.427	0.442	0.718	0.714	0.522	0.932
rms deviation		±0.350		±0.330		±0.910		±0.565	

ing 2.0 mol% of Nd^{3+}. It indicates that the non-symmetric component of the electric field acting on Nd^{3+} ion is low for 0.5 mol% Nd^{3+} glass and is strong for 2.0 mol% Nd^{3+} glass. The Judd-Ofelt intensity parameters (Ω_2, Ω_4 and Ω_6) which are obtained from the experimental oscillator strengths are presented in Table 3. These parameters depend on host glass composition [15]. Normally, Ω_2 indicate covalencey of metal ligand bond and Ω_4 and Ω_6 are related to the rigidity of the host matrix. In the present work, Ω_2 exhibits a maximum for 0.5 mol% of Nd^{3+} doped glass and a minimum for 1.5 mol% of Nd^{3+} glass. It indicates that high covalency (low ionicity) between neodymium cation and oxide anion and to a relatively high symmetry of the local surroudings of the neodymium ion in 0.5 mol% Nd^{3+} glass. The differences in Ω_2 parameter should therefore be attributed to the dominant site symmetry and covalency effects. Ω_4 and Ω_6 values exhibit minimum in 0.5 mol% of Nd^{3+} glass and maximum in 2.0 mol% of Nd^{3+} glass.

For Nd^{3+} ion, $^4I_{9/2} \rightarrow {}^4G_{5/2} + {}^2G_{7/2}$ is the hypersensitive transition. It will follow the selection rules, $\Delta J \leq 2$, $\Delta L \leq 2$ and $\Delta S = 0$. Normally the intensity parameter Ω_2 which indicates covalency, decreases or increases with the intensity of the hypersensitive transition [16]. In the present work also, the Ω_2

Table 3 Judd-Ofelt intensity parameters ($\Omega_\lambda \times 10^{20}$) (in cm^2) in potassium borate glass with different Nd^{3+} concentrations and in other glass matrices.

Glass matrix	Ω_2	Ω_4	Ω_6	$\Sigma\Omega_\lambda$	Ref.
$0.5Nd_2O_3 + 19.5K_2CO_3 + 80H_3BO_3$	7.19 ± 0.65	3.30 ± 0.29	3.70 ± 0.25	14.19	present work
$1.0Nd_2O_3 + 19.0K_2CO_3 + 80H_3BO_3$	6.30 ± 0.55	3.29 ± 0.30	4.24 ± 0.48	13.84	present work
$1.5Nd_2O_3 + 18.5K_2CO_3 + 80H_3BO_3$	4.56 ± 0.40	5.34 ± 0.52	3.75 ± 0.30	13.65	present work
$2.0Nd_2O_3 + 18.0K_2CO_3 + 80H_3BO_3$	5.56 ± 0.52	6.99 ± 0.71	5.21 ± 0.50	17.76	present work
$30Na_2O + 70B_2O_3$	4.91	3.28	4.51	12.70	[20]
$30K_2O + 70B_2O_3$	4.94	3.10	3.42	11.46	[20]
$30PbO + 70B_2O_3$	3.96	3.77	4.88	12.61	[15]
$30Li_2O + 70B_2O_3$	4.20	3.89	4.74	12.83	[21]
$30Ca_2O + 70B_2O_3$	3.43	3.45	3.15	10.03	[21]

parameter decreases with the decrease of intensity of hypersensitive transition for 0.5, 1.0 and 1.5 mol% of Nd^{3+} glasses. Instead of observing the variation of Ω_2 alone with the intensity of hypersensitive transition, Oomen and Van Dongen [17] suggested that the intensity of the hypersensitive transition vary with the sum of the intensity parameters ($\Sigma\Omega_\lambda$). In the present work, $\Sigma\Omega_\lambda$ decreases with the decrease of intensity of hypersensitive transition. The Judd-Ofelt intensity parameters Ω_2, Ω_4 and Ω_6 and the sum of the intensity parameters ($\Sigma\Omega_\lambda$) for all these glasses along with the other different hosts are presented in Table 3. From the table it is observed that $\Sigma\Omega_\lambda$ values decreases with increasing average molecular weight of the glass i.e., for Li, Na, K and Ca borate glasses. But for lead borate glass it was not followed.

The peak to peak separation between the hypersensitive $^4G_{5/2} \rightarrow {}^4I_{9/2}$ transition and the $^2G_{7/2} \rightarrow {}^4I_{9/2}$ transition in all the absorption spectra of Nd^{3+} doped glasses decreases with increasing of Nd^{3+} concentration. Judd [18] suggests that the appearance of the spectral profile of the hypersensitive transition is strongly affected by changes in the symmetry of the crystalline field acting on the rare earth ion. A difference in the shape of this transition indicates a difference in the environment of Nd^{3+} ion. In the present work, though the spectral profiles of the hypersensitive transition shows small changes for different rare earth ion concentrations, the other two bands showing differences in the spectral profiles for different concentrations thus conforming that the crystal field asymmetry is different. Similar results have been observed by Gatterer et al. [16] in the case of sodium borate and sodium silicate glasses.

4.4 Radiative properties

Electric dipole line strengths (S_{ed}), radiative transition probabilities (A_{rad}), radiative lifetimes (τ_R), branching ratios (β) and integrated absorption cross sections (Σ) for the excited states $^4G_{9/2}$,$^4G_{7/2}$, $^4G_{5/2}$, $^2H_{11/2}$, $^4F_{9/2}$, $^4F_{5/2}$ and $^4F_{3/2}$ of Nd^{3+} ion have been calculated. Table 4 gives total radiative transition probabilities and radiative lifetimes of all the above excited states. The radiative lifetimes of the excited states $^4G_{9/2}$,$^4G_{7/2}$, $^4G_{5/2}$ and $^2H_{11/2}$ are slightly increasing with the increase of Nd^{3+} for 0.5, 1.0 and 1.5 mol% concentrations. But for 2 mol% of Nd^{3+}, lifetime values are decreased. The radiative lifetimes of the above excited states are lower in the case of 2.0 mol% of Nd^{3+} concentration. For $^4F_{9/2}$, $^4F_{5/2}$ and $^4F_{3/2}$ excited states, the lifetimes are decreased with the increase of rare earth ion concentration. In fluoroarsenate glass [19] also, the radiative lifetime of the excited level, $^4F_{3/2}$ is decreasing with the increase of Nd^{3+} concentration at room temperature, at 4.2 K and also at 77 K. The increase in lifetimes with increasing Nd^{3+} concentration may be attributed to radiation trapping, and the decrease in lifetimes with Nd^{3+} concentration may result from concentration quenching. The branching ratio, β is given by A/A_T, where A is the transition probability for the transition and A_T is the total transition probability from the relevant excited state. A higher β signifies a higher stimulated emission cross section. $^4F_{3/2} \rightarrow {}^4I_{11/2}$ transition is widely used lasing transition. This transition shows the largest

Table 4 Total radiative transition probabilities (A_T) (in s^{-1}) and radiative lifetimes (τ_R) (in μs) of certain excited states of Nd^{3+} in potassium borate glass with different Nd^{3+} concentrations.

Serial No.	Excited level	0.5 mol%		1.0 mol%		1.5 mol%		2.0 mol%	
		A_T	τ_R	A_T	τ_R	A_T	τ_R	A_T	τ_R
1.	$^4G_{9/2}$	11032	91	10509	95	10312	97	13391	75
2.	$^4G_{7/2}$	10979	91	10269	97	9592	104	12230	82
3.	$^4G_{5/2}$	17358	58	16081	62	15089	66	18934	53
4.	$^2H_{11/2}$	419	2385	394	2535	367	2724	458	2183
5.	$^4F_{9/2}$	2011	497	2244	445	2333	428	3156	317
6.	$^4F_{5/2}$	2467	405	2686	372	3055	327	4032	248
7.	$^4F_{3/2}$	1893	528	2048	488	2425	412	3175	315

Table 5 Branching ratios (β) and integrated absorption cross sections (Σ) (in cm^{-1}) of certain transitions of Nd^{3+} in potassium borate glass with different Nd^{3+} concentrations.

Serial No.	Transition	0.5 mol%		1.0 mol%		1.5 mol%		2.0 mol%	
		β	Σ	β	Σ	β	Σ	β	Σ
1.	$^4G_{9/2} \rightarrow {}^4I_{13/2}$	0.588	16.18	0.565	14.61	0.496	12.76	0.484	16.02
2.	$^4G_{7/2} \rightarrow {}^4I_{11/2}$	0.648	14.29	0.622	12.73	0.518	10.04	0.504	12.41
3.	$^4G_{5/2} \rightarrow {}^4I_{9/2}$	0.864	29.45	0.848	26.63	0.796	23.74	0.788	29.67
4.	$^4F_{5/2} \rightarrow {}^4I_{9/2}$	0.660	6.06	0.660	6.62	0.645	7.38	0.643	9.91
5.	$^4F_{3/2} \rightarrow {}^4I_{9/2}$	0.418	3.54	0.397	3.64	0.483	5.26	0.476	6.88
6.	$^4F_{3/2} \rightarrow {}^4I_{11/2}$	0.488	6.04	0.503	6.72	0.441	6.99	0.447	9.43
7.	$^4F_{3/2} \rightarrow {}^4I_{13/2}$	0.090	1.84	0.096	2.11	0.072	1.87	0.074	2.56
8.	$^4F_{3/2} \rightarrow {}^4I_{15/2}$	0.004	0.17	0.005	0.20	0.003	0.18	0.003	0.25

β value in 1.0 mol% of Nd^{3+} potassium borate glass. Branching ratios (β) and integrated absorption cross sections (Σ) of certain transitions which have larger magnitudes are collected in Table 5. From the table, it is observed the branching ratios of the transitions $^4G_{9/2} \rightarrow {}^4I_{13/2}$, $^4G_{7/2} \rightarrow {}^4I_{11/2}$, $^4G_{5/2} \rightarrow {}^4I_{9/2}$ and $^4F_{5/2} \rightarrow {}^4I_{5/2}$ are decreasing with increasing Nd^{3+} concentration.

4.5 Luminescence spectra

The luminescence spectrum of Nd^{3+} doped potassium borate glass with 1.5 mol% of Nd^{3+} concentration in the region 800–1500 nm under excitation wavelength 514 nm of Ar^{3+} laser is shown in Fig. 2. The spectra of other concentrations are not shown as they are in similar shape. In the emission spectra of Nd^{3+}, a broad band at 880 nm, a strong band at 1058 nm and another band at 1330 nm are identified. These bands are assigned to the transitions $^4F_{3/2} \rightarrow {}^4I_{9/2}$, $^4F_{3/2} \rightarrow {}^4I_{11/2}$ and $^4F_{3/2} \rightarrow {}^4I_{13/2}$. The observed luminescence spectrum consists of overlapping lines arising from transitions between the split $^4F_{3/2}$ level and various sub levels of $^4I_{9/2}$, $^4I_{11/2}$ and $^4I_{13/2}$ states. It is observed that as the concentration increases, the fine structure splitting of peaks increases for 0.5, 1.0 and 1.5 mol% but for 2.0 mol%

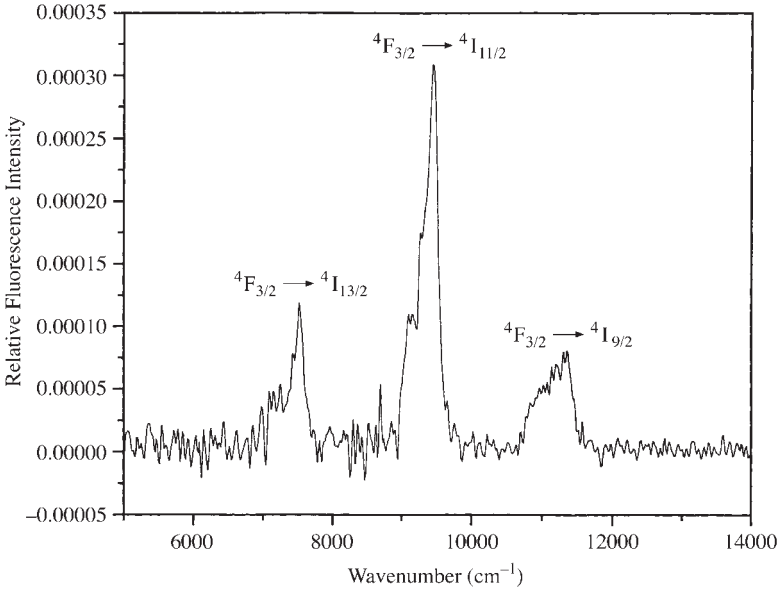

Fig. 2 Luminescence spectrum of Nd^{3+} doped potassium borate glass with 1.5 mol% Nd^{3+} concentration.

Table 6 Certain fluorescent properties of Nd^{3+} doped potassium borate glass with different concentrations.

Serial No.	Concentration	$^4F_{3/2} \rightarrow {}^4I_{9/2}$					$^4F_{3/2} \rightarrow {}^4I_{11/2}$					$^4F_{3/2} \rightarrow {}^4I_{13/2}$				
		λ_p (nm)	A_{rad} (s^{-1})	$\Delta\lambda$ (cm^{-1})	σ_p (10^{-20} cm^2)	β	λ_p (nm)	A_{rad} (s^{-1})	$\Delta\lambda$ (cm^{-1})	σ_p (10^{-20} cm^2)	β	λ_p (nm)	A_{rad} (s^{-1})	$\Delta\lambda$ (cm^{-1})	σ_p (10^{-20} cm^2)	β
1.	0.5 mol%	882	791	562	0.632	0.209	1055	923	309	1.922	0.588	1329	170	277	0.627	0.202
2.	1.0 mol%	882	813	519	0.710	0.218	1061	1029	308	2.181	0.577	1329	197	299	0.673	0.203
3.	1.5 mol%	882	1172	558	0.953	0.221	1061	1070	301	2.329	0.571	1333	174	291	0.621	0.207
4.	2.0 mol%	890	1513	580	1.204	0.189	1060	1418	336	2.769	0.593	1337	233	351	0.694	0.217

the peak splittings are lower. It shows the structural variations and the accompanying changes in the Nd-O bonding. Similar results have been observed from the spectral profiles of the hypersensitive transition.

The intensity parameters obtained from the optical absorption spectra have been used to determine the radiative properties. Table 6 gives peak wavelengths (λ_p), radiative transition probabilities (A_{rad}), effective bandwidths ($\Delta\lambda_{eff}$), stimulated emission cross sections (σ_p) and measured branching ratios (β) for the $^4F_{3/2} \rightarrow {}^4I_{9/2}$, $^4F_{3/2} \rightarrow {}^4I_{11/2}$ and $^4F_{3/2} \rightarrow {}^4I_{13/2}$ transitions. The emission band, $^4F_{3/2} \rightarrow {}^4I_{11/2}$ at 1058 nm has been considered as potential lasing transition due to the large stimulated emission cross-section. An efficient laser transition is characterized by large stimulated emission cross-section. The σ_p values increase with increasing Nd^{3+} concentration for the $^4F_{3/2} \rightarrow {}^4I_{9/2}$ and $^4F_{3/2} \rightarrow {}^4I_{11/2}$ transitions. σ_p value is more in the case of 2.0 mol% of Nd^{3+} glass and less in the case of 0.5 mol% of Nd^{3+} glass. The observed branching ratio (β) is also more in the case of 2.0 mol% of Nd^{3+} concentration. Hence, the potassium borate glass consisting 2.0 mol% Nd^{3+} is more suitable for lasing material.

5 Conclusions

The optical band gap values (E_{opt}) for indirect transitions are decreased with increasing Nd^{3+} concentration in potassium borate glass. The Judd-Ofelt theory is found to describe well the spectral intensities of the transitions of Nd^{3+} in this glass. The higher value of Ω_2 parameter indicates higher covalency between the neodymium cation and the oxide anions in 0.5 mol% Nd^{3+} doped glass. From the spectral profiles of the hypersensitive transition, it is observed that the environment of Nd^{3+} ion is slightly different for different Nd^{3+} concentrations. The radiative transition probabilities, radiative lifetimes and branching ratios are calculated using the intensity parameters obtained from the absorption spectra. Radiative lifetimes of certain excited states decrease with increasing rare earth ion concentration. The lifetimes are minimum in the case of 2.0 mol% of Nd^{3+} in potassium borate glass. Branching ratios and integrated absorption cross sections are compared for certain transitions of Nd^{3+} in all the glasses. From the luminescence spectra, peak wavelengths, observed branching ratios and emission cross sections are obtained for the three transitions $^4F_{3/2} \rightarrow {}^4I_{9/2}$, $^4F_{3/2} \rightarrow {}^4I_{11/2}$ and $^4F_{3/2} \rightarrow {}^4I_{13/2}$. Emission cross section values are increased with the increase of Nd^{3+} concentration for the $^4F_{3/2} \rightarrow {}^4I_{11/2}$ and $^4F_{3/2} \rightarrow {}^4I_{13/2}$ transitions.

Acknowledgements The author YCR expresses his thanks to UGC for providing the financial assistance in the form of research scheme. He also expresses his thanks to the Head, Department of Physics, S.V.U.P.G. Centre, Kavali for providing the necessary facilities in execution of the above work.

References

[1] M. Dejneka and B. Samson, Mater. Res. Bull. **24**, 39 (1999).
[2] M. J. Weber, J. Non-Cryst. Solids **42**, 189 (1980).
[3] B. R. Judd, Phys. Rev. **127**, 750 (1962).
[4] G. S. Ofelt, J. Chem. Phys. **37**, 511 (1962).
[5] K. Binnemans, R. van Deun, C. Gorller-Walrand, and J. L. Adam, J. Alloys Compd. **275**, 455 (1998).
[6] H. Li, L. Li, J. D. Vienna, M. Qian, Z. Wang, J. G. Darab, and D. K. Peeler, J. Non-Cryst. Solids **278**, 35 (2000).
[7] K. Lu and N. K. Dutta, J. Appl. Phys. **89**, **6**, 3079 (2001).
[8] M. Naftaly and A. Jha, J. Appl. Phys. **87**, **5**, 2098 (2000).
[9] G. K. Das Mohapatra, Phys. Chem. Glasses **40**, 12 (1999).
[10] V. V. Ravi Kanth Kumar and Anil K. Bhatnagar, Opt. Mater. **11**, 41 (1998).
[11] Y. C. Ratnakaram and A. Viswanadha Reddy, J. Non-Cryst. Solids **277**, 142 (2000).
[12] Y. C. Ratnakaram and N. Sudharani, J. Non-Cryst. Solids **217**, 291 (1997).
[13] N. F. Mott and E. A. Davis, Electronic Processes in Non-Cryst. Materials, second ed. (Oxford University Press, Oxford, 1979).
[14] E. Y. Wong, J. Chem. Phys. **35**, 544 (1961).
[15] M. B. Saisudha and J. Ramakrishna, Phys. Rev. B **53**, 6186 (1996).
[16] K. Gatterer, G. Pucker, H. P. Fritzer, and S. Arafa, J. Non-Cryst. Solids **176**, 237 (1994).
[17] E. W. J. L. Oomen and A. M. A. van Dongen, J. Non-Cryst. Solids **111**, 205 (1989).
[18] B. R. Judd, J. Chem. Phys. **44**, 839 (1966).
[19] J. L. Adam, R. Balda, I. Melscoet, F. Smektala, L. M. Lacha, and J. Fernandez, J. Non-Cryst. Solids **256/ 257**, 390 (1999).
[20] H. Takebe, K. Morinaga, and T. Izumitani, J. Non-Cryst. Solids **178**, 58 (1994).
[21] P. Nachimuthu, P. Harikishan, and R. Jagannathan, Phys. Chem. Glasses **38**, 59 (1997).